

adopted a type of structure as shown in Fig. 5, much similar to the type adopted for the quadrupole. Differing from the quadrupole, however, the mechanical structure of the vertical steering is not necessarily so strong as the quadrupole is, so that one of the side yokes is made open to let SR pass through. Two-dimensional calculation of LINDA implied that the field degraded by splitting the side yokes could be restored by attaching four rectangular shims, each about 10 mm wide and 10 mm high, to the inside wall of the

Table I. Principal parameters of the magnets

| Quadrupole | |
|--------------------------------|---------------------|
| gradient (B') | 9.5 T/m |
| main coil current | 500 A |
| turn number of coil | 23 per pole |
| bore radius | 55 mm |
| length of iron core | 0.5 m |
| width of iron yoke | 100 mm |
| electric resistance | 32 mΩ |
| cooling water | 5 l/min. |
| power dissipation | 8 kW |
| correction coil current | 4.5 A (max.) |
| number of correction coils | 4 |
| turn number of correction coil | 100 per coil |
| Sextupole | |
| sextupole gradient (B'') | 29 T/m ² |
| current | 3 A (max. 5 A) |
| turn number of coil | 436 per pole |
| bore radius | 70 mm |
| length of iron core | 0.2 m |
| electric resistance | 9.5 Ω |
| power dissipation | 85 W (max. 240 W) |
| diameter of conductor | 1.8 mm |
| Vertical steering | |
| field (B) | 380 G |
| current | 3 A |
| turn number of coil | 2100 per pole |
| length of iron core | 80 mm |
| electric resistance | 14 Ω |
| power dissipation | 127 W |
| diameter of conductor | 1.6 mm |

iron yokes. As the length of magnet is shorter than the transverse dimensions, however, various sizes of shims were prepared to choose an optimum size in the field measurement.

III. Field Measurement

The magnetic field measurements were carried out mainly using the following two methods; (1) a moving induction coil for the quadrupole and (2) harmonic coils for the sextupole and the vertical steering. Furthermore, a rotating coil was used for quadrupole and sextupole to check the reliability of measurement made by the above methods, and also used was a colloidal instrument to measure the magnetic centers³. In the method (1), at the same time that a horizontal position of the moving coil was measured with a precision of 50 μm by a Nikon position scale, the voltage induced by the quadrupole field was also measured with 1×10⁻⁴ accuracy by VFC (Voltage to Frequency Converter) connected to a CAMAC scaler system.

For the quadrupole, a good field region (about ±40 mm) of the integrated gradient distribution as shown in Fig. 6 was obtained by attaching a pair of end shims at each end of the pole pieces. The thickness of the end shims was chosen to be 4 mm. The excitation current was measured up to 800 A (beyond a maximum-allowed current of 500 A), and compared with that of an existing quadrupole of Type I (see Fig. 7). The difference in excitation that became apparent above 300 A (0.7% at 300 A and 4.0% at 800 A) was compensated for by exciting the correction coil. The correction current required for compensation is plotted with respect to the main current in Fig. 8, and it is only 1.0 A at the ring energy of 2.5 GeV. The magnetic center was checked using a colloidal instrument³ and agreed with a geometric center less than 50 μm below a current of 400A, though it was slightly deviated with the correction coil current as shown in Fig. 9. A large deviation seen in the figure at a high current that had also been observed for the existing Type I quadrupoles is due to the iron support legs, which give rise to an asymmetry in the magnetic circuit of the quadrupole.

The mechanical distortion due to magnetic stress was measured by strain gauges directly stuck on the magnet and by those stuck on pieces of aluminum that were in turn fixed between the minimum gaps in the magnet. The latter gauges had a better sensitivity and gave the same order of strain as predicted. Temperature rise and flow rate of the cooling water were measured simultaneously, and the flow rate was observed to increase with the current due to the

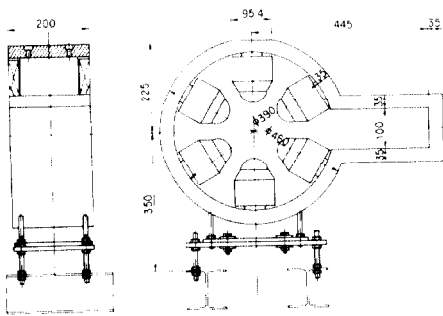


Fig. 4 Design sketch of the sextupole. The whole yoke is made of iron.

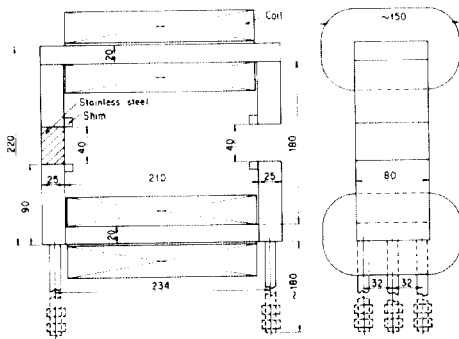


Fig. 5 Design sketch of the vertical steering. The shaded portion is made of stainless steel.

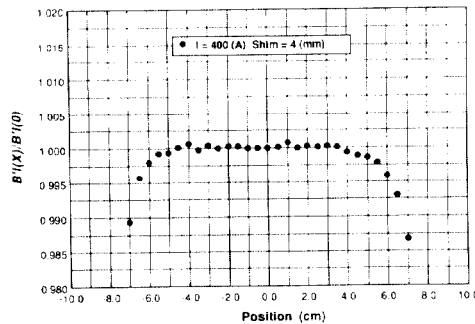


Fig. 6 Integrated gradient distribution $B'l(x)/B'l(0)$ versus the horizontal position (x) of the quadrupole at a current of 400 A with 4 mm-thick end shims.

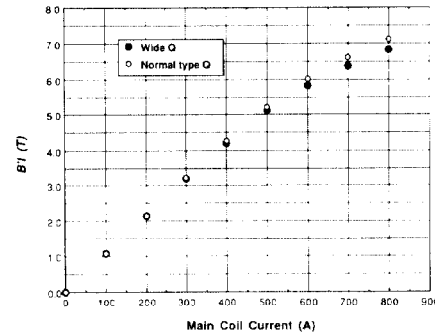


Fig. 7 Comparison of the excitation curves between the quadrupole and one of the existing quadrupoles (Type I). Wide Q and Normal type Q in the figure indicate the designed magnet and a magnet of Type I, respectively.

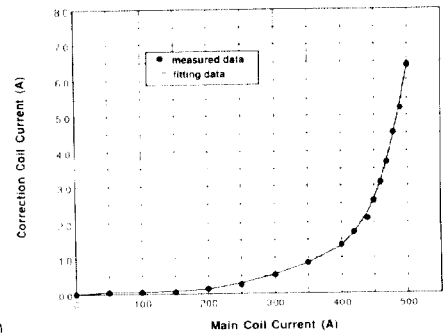


Fig. 8 Correction coil current required to compensate for the difference in excitation.

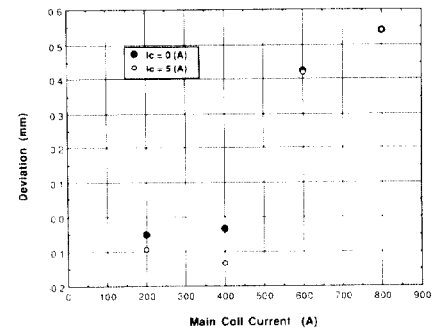


Fig. 9 Deviation of the magnetic center of the quadrupole versus the main coil current.

temperature dependence of the viscosity of water. The details of both strain and temperature measurements will be reported elsewhere.

The field strength of the sextupole measured by a harmonic coil is $B''l = 10.13$ T/m at 4.5 A, and the field distribution measured by a rotating coil is shown in Fig. 10. Further the field around the center of magnet was finely measured and found that the field has an opposite sign to that of the outer region, just as predicted by the field calculation.

For the vertical steering, the 10 mm-thick end shims were as optimum in the field measurement as in the two-dimensional calculation. The distribution of the integrated field is shown in Fig. 11 and the field strength is $B_l = 73.4$ G-m at a current of 3.0 A.

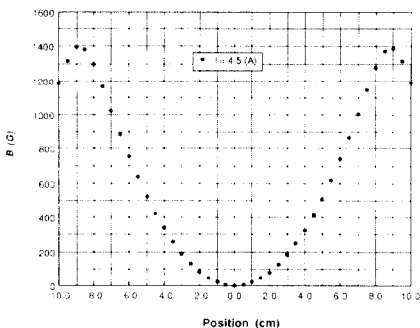


Fig. 10 Field distribution at the center of the sextupole measured by a rotating coil.

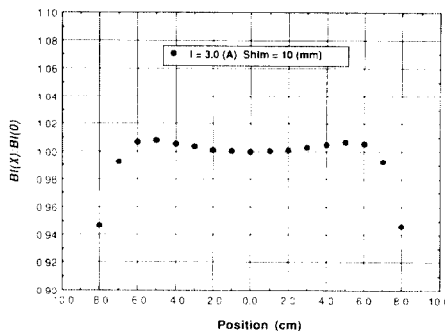


Fig. 11 Integrated field distribution of the vertical steering.

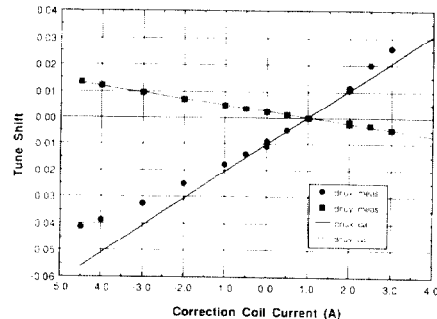


Fig. 13 Tune shift versus the correction coil current. Closed circles denote the measured values and solid line the expected value.

IV. Effects on Beam Orbit

The effects of the magnets on the beam orbit were studied after installing the magnets at the downstream of a bending magnet called B22, which was actually impossible to use for SR experiment because of the building structure. Since the quadrupole is a horizontally focusing magnet, the effects on the tune shift and the distortion of betatron function appeared more clearly in the horizontal direction than in the vertical direction, when the current of the correction coil in the quadrupole was set to a value different from the nominal one determined by the field measurement. Figure 12 shows the measured beta functions for three different values of the

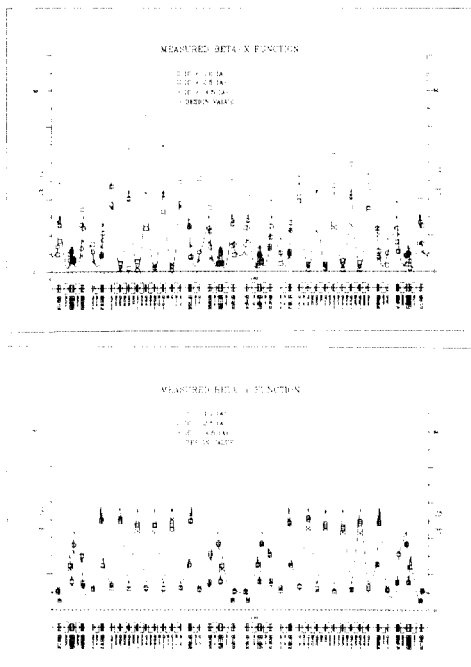


Fig. 12 Measured beta functions. Closed circles for a correction coil current of 1.0 A, open squares for 2.5 A, cross symbols for -4.5 A and the solid line for the design value.

correction coil current (1.0, 2.5 and -4.5 A) and Fig. 13 shows the tune shifts with respect to the correction current. The method of measuring beta function is described in Ref. 4. At the nominal current of 1.0 A, both horizontal and vertical beta functions agreed well with the design values and any appreciable tune shifts were not observed. As shown in Fig. 14, the beta distortion measured at the other values of the correction coil current was also in good agreement with the distortion predicted from the data of field measurement.

The closed orbit distortion produced by the deviation of the magnetic centers in the quadrupole and in the sextupole was found to be negligibly small. The chromaticities were also measured and any appreciable change from the previous values was not found.

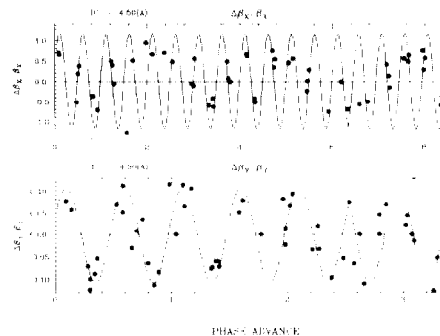


Fig. 14 Fractional changes of the beta functions at -4.5 A for the correction coil. Closed circles denote the measured values and solid lines the expected values.

V. Summary and Acknowledgements

The magnets described here are being operated without any trouble until now, while a kind of antechamber appropriate for the magnets will be installed within a few years⁵⁾. If the magnets and vacuum chamber together achieve their design specifications, next step is probably "the full moon project" which will utilize the unused bending magnets in the injection region for supplying SR with extraction angles much wider than previously available.

We would like to thank all staff of the Light Source Division of the Photon Factory, in particular, Prof. M. Kobayashi and Dr. Y. Hori for their discussion about the vacuum chamber yet to be installed in the magnets. We also thank Prof. R. Sugahara of the Accelerator Department for kindly lending us his colloidal instrument.

References

- (1) for example see the ESRF Design Report "RED BOOK", January 1987, the ALS Conceptual Design Report, July 1986 and so on.
- (2) KEK version of the program LINDA, and also see K. Endo and M. Kihara, "Manual of Magnetostatic program LINDA", KEK ACCELERATOR-1, 1972 (in Japanese).
- (3) R. Sugahara, T. Kubo and Y. Oosawa, "A Colloidal Solution of Fe_3O_4 Crystallites to Optically Locate the Magnetic Center of Multipole Magnets", KEK Report 89-9, September 1989.
- (4) I. Honjo, M. Katoh, A. Araki, Y. Kamiya, and M. Kihara, "Measurement of Betatron Function at the Photon Factory", in Proc. of the 1987 IEEE Part. Accel. Conf., p. 1272, 1987.
- (5) M. Kobayashi and Y. Hori, private communication.